Critical Signaling Events in the Mechanoactivation of Human Mast Cells through p.C492Y-ADGRE2

Andrea N. Naranjo[1], Geethani Bandara[1], Yun Bai[1], Margery G. Smelkinson[2], Araceli Tobío[1], Hirsh D. Komarow[1], Steven E. Boyden[3], Daniel L. Kastner[3], Dean D. Metcalfe[1] and Ana Olivera[1]

A role for the adhesion G-protein coupled receptor ADGRE2 or EMR2 in mechanosensing was revealed by the finding of a missense substitution (p.C492Y) associated with familial vibratory urticaria. In these patients, friction of the skin induces mast cell hyper-degranulation through p.C492Y-ADGRE2, causing localized hives, flushing, and hypotension. We have now characterized the responses and intracellular signals elicited by mechanical activation in human mast cells expressing p.C492Y-ADGRE2 and attached to dermatan sulfate, a ligand for ADGRE2. The presence of p.C492Y-ADGRE2 reduced the threshold to activation and increased the extent of degranulation along with the percentage of mast cells responding. Vibration caused phospholipase C activation, transient increases in cytosolic calcium, and downstream activation of phosphoinositide 3-kinase and extracellular signal–regulated kinases 1 and 2 by Gβγ, $G\alpha_{q/11}$, and $G\alpha_{i/o}$-independent mechanisms. Degranulation induced by vibration was dependent on phospholipase C pathways, including calcium, protein kinase C, and phosphoinositide 3-kinase but not extracellular signal–regulated kinases 1/2 pathways, along with pertussis toxin-sensitive signals. In addition, mechanoactivation of mast cells stimulated the synthesis and release of prostaglandin D_2, to our knowledge a previously unreported mediator in vibratory urticaria, and extracellular signal–regulated kinases 1/2 activation was required for this response together with calcium, protein kinase C, and to some extent, phosphoinositide 3-kinase. Our studies thus identified critical molecular events initiated by mechanical forces and potential therapeutic targets for patients with vibratory urticaria.

Journal of Investigative Dermatology (2020) ■, ■–■; doi:10.1016/j.jid.2020.03.936

INTRODUCTION

Adhesion G-protein coupled receptors (aGPCRs) represent the second largest class of receptors within the GPCR superfamily. They are involved in cell-to-cell and cell-to-matrix interactions and are thought to play important roles in immunity, tumorigenesis, reproduction, and development (Langenhan et al., 2013). ADGRE2 or EMR2 is an aGPCR that binds dermatan sulfate (DS) (Stacey et al., 2003) and is predominantly expressed in human myeloid cells.

ADGRE2 regulates neutrophil function and survival (Chen et al., 2011; Yona et al., 2008) and induces macrophage differentiation and expression of proinflammatory mediators (I et al., 2017, Kwakkenbos et al., 2002). Recently, we found that ADGRE2 is expressed in human mast cells and that a missense variant (p.C492Y) of ADGRE2 identified in patients with autosomal dominant vibratory urticaria (VU) is associated with disease presentation. These patients exhibit mast cell hyperreactivity on mechanical stimuli, resulting in localized hives, increased histamine levels in serum, and increased extracellular tryptase staining in the dermis. Vibratory stimulation in vitro causes degranulation of mast cells derived from patients' progenitors, and enforced expression of the p.C492Y-ADGRE2 variant in mast cells reproduces this phenotype. These results provide a link between p.C492Y-ADGRE2 and vibration-induced mast cell degranulation and support a function for this receptor in sensing physical forces (Boyden et al., 2016), as has been reported for other aGPCR family members (Purcell and Hall, 2018; Scholz et al., 2016). However, the intracellular signals activated by mechanical stimulation of ADGRE2 and other aGPCRs remain elusive.

In this study, we investigated the mechanisms of p.C492Y-ADGRE2 activation in mast cells with the dual purpose of identifying the signals causing the pathologic presentation of VU and gaining insights into vibration-induced signal transduction that may be common to other mechanosensing aGPCRs. We show that ADGRE2 activation by physical stimulation, particularly the p.C492Y variant, assembles

[1]*Mast Cell Biology Section, Laboratory of Allergic Diseases, National Institute of Allergy and Infectious Diseases, National Institutes of Health, Bethesda, Maryland, USA;* [2]*Biological Imaging Section, National Institute of Allergy and Infectious Diseases, National Institutes of Health, Bethesda, Maryland, USA; and* [3]*Inflammatory Disease Section, National Human Genome Research Institute, National Institutes of Health, Bethesda, Maryland, USA*

Correspondence: Ana Olivera, Mast Cell Biology Section, Laboratory of Allergic Diseases, National Institute of Allergy and Infectious Diseases, National Institutes of Health, 10 Center Drive, Bethesda, Maryland 20892, USA. E-mail: ana.olivera@nih.gov

Abbreviations: aGPCR, adhesion G-protein coupled receptors; Akt, protein kinase B; AU, arbitrary units; DAG, diacylglycerol; DS, dermatan sulfate; ERK, extracellular signal–regulated kinase; HEPES, 4-(2-hydroxyethyl)-1-piperazineethanesulfonic acid; LAD2, laboratory of allergic diseases-2 human mast cell line; MEK, MAPK/ERK kinase; NM, nonmutated; NTF, N-terminal fragment; PGD_2, prostaglandin D_2; PTX, pertussis toxin; PI3K, phosphoinositide 3-kinase; PKC, protein kinase Cl; PLC, phospholipase C; VU, vibratory urticaria

Received 15 November 2019; revised 18 February 2020; accepted 3 March 2020; accepted manuscript published online XXX; corrected proof published online XXX

functionally distinct signaling events that enhance sensitivity to vibration. Vibration-induced signals include activation of phospholipase C (PLC) and calcium mobilization, which were essential for downstream activation of phosphoinositide 3-kinase (PI3K) and extracellular signal–regulated kinase (ERK) 1/2 pathways. Although calcium and protein kinase C (PKC) were required for degranulation, ERK1/2 pathways were essential for the release of prostaglandin D_2 (PGD_2), which increased in serum of patients with VU after vibratory challenge. Our data contribute to the understanding of the pathways activated by aGPCR-mediated mechanosensing and identify potential therapeutic targets for treatment of patients with VU.

RESULTS AND DISCUSSION

Characterization of vibration-induced degranulation

We sought to further characterize the responses to physical stimulation using the laboratory of allergic diseases-2 human mast cell line (LAD2) transfected with normal or mutated *ADGRE2* (Figure 1a), which resulted in similar efficiencies of transfection (>70%; Supplementary Figure S1a) (Boyden et al., 2016). We first examined the effect of vibratory stimuli of various strengths in cells attached to DS on the release of β-hexosaminidase as a read-out for degranulation. Speeds lower than 1,500 r.p.m. caused minor degranulation in cells expressing nonmutated (NM)-ADGRE2, whereas cells expressing p.C492Y-ADGRE2 readily degranulated at 750 r.p.m. or higher (Figure 1b and c; Supplementary Figure S1b, d, and e). Optimal differences in degranulation between the two variants were observed between 750 and 1,500 r.p.m., whereas higher stimulus strengths caused substantial degranulation in all cells, diminishing the differences between variants (Figure 1c), a result that was not because of cellular damage as viability was >90% after vibration at 2,000 r.p.m. (Supplementary Figure S1c). In agreement with clinical observations in VU, the results demonstrate that the p.C492Y-ADGRE2 variant requires lower threshold for activation of mast cells in response to vibration.

To gain further insights into the heterogeneity of individual cell degranulation to vibration, we monitored the exposure of the granule marker CD63 onto the cell surface using confocal microscopy. This method efficiently showed increased cell surface expression of CD63 during degranulation in cells stimulated with thapsigargin or with IgE and antigen (Supplementary Figure S2a and b). Vibration also increased anti-CD63 surface staining, particularly on cells expressing p.C492Y-ADGRE2 (Figure 1d and e), although an increase was also seen in cells with NM-ADGRE2 at higher speeds (Supplementary Figure S2c). Similar to β-hexosaminidase release (Figure 1b and c), stronger mechanical stimulation reduced the differences in CD63 expression between NM-ADGRE2 and p.C492Y-ADGRE2 variants (Supplementary Figure S2c). Analysis of responding cells (i.e., cells showing CD63 surface staining above background) indicated that both the magnitude of degranulation on a per cell basis (Figure 1f) and the percentage of responding cells (Figure 1g) were markedly increased when expressing p.C492Y-ADGRE2.

Degranulation was observed when p.C492Y-ADGRE2 cells were attached to immobilized DS, a reported ligand for ADGRE2 (Stacey et al., 2003) or 2A1, an antibody that recognizes a sequence in the N-terminal fragment (NTF) (Figure 1a) and ligates the receptor in macrophages (Huang et al., 2012), but not to chondroitin sulfate A, an analog of DS, polylysine, hyaluronic acid, or heparan sulfate (Supplementary Figure S1d). These and our reported findings (Boyden et al., 2016) suggest that binding of ADGRE2 to immobilized DS or to 2A1 is required, along with mechanical forces, to elicit degranulation in mast cells because in static conditions, no significant degranulation occurred (Figure 1b). Vibration-induced responses in p.C492Y-ADGRE2 cells were similar at concentrations of immobilized DS ranging from 0.1 μg/ml to 100 μg/ml (Supplementary Figures S1e and S3c), consistent with the observed maximal adherence of cells to DS within this range (Boyden et al., 2016). In other mechanosensing aGPCRs, activation is also thought to require both ligation and a mechanical load, as ligand binding by itself causes no detectable signaling (Karpus et al., 2013; Langenhan et al., 2013; Scholz et al., 2015) or inhibits signaling (Petersen et al., 2015). A proposed model of activation of aGPCRs suggests that the NTF normally prevents spontaneous activation and that dissociation of the NTF from the C-terminal fragment (Figure 1a) is required for signaling to occur (Purcell and Hall, 2018; Scholz et al., 2016). Consistent with this model, the presence of p.C492Y destabilized the noncovalent interaction between the NTF and C-terminal fragment in mast cells, rendering the receptor more susceptible to dissociating the NTF after a vibratory stimulus (Boyden et al., 2016), a hypothesis also consistent with the lower threshold of activation in cells with p.C492Y (Figure 1b; Supplementary Figure S1b) and recent results showing that proteolytic clipping of the NTF of ADGRE2 by α/β-tryptase heterotetramers makes mast cells susceptible to vibration-triggered degranulation (Le et al., 2019).

Vibration causes calcium mobilization in mast cells

Although other aGPCR members have also been viewed as mechanosensors (Scholz et al., 2016), there is limited information on how such receptors signal. Calcium is viewed as one potential messenger in aGPCR-mediated mechanosensing (Clapham, 2003; Scholz et al., 2016, 2015) and also a critical signal for mast cell degranulation (Gilfillan and Tkaczyk, 2006). Following this lead, we determined that in mast cells loaded with Fura-2-acetoxymethyl ester, vibration induced a rise in cytosolic calcium, particularly in p.C492Y-ADGRE2 cells, which was maximal immediately after vibration (∼0.85 μM in NM-ADGRE2 cells and ∼1.5 μM in p.C492Y-ADGRE2 cells) and declined thereafter (Figure 2a). These transient calcium spikes resembled the typical transient calcium mobilization reported to occur after GPCR activation in mast cells. GPCR-induced calcium responses are associated with a distinct degranulation pattern that causes rapid and brief vascular reactions in vivo (Gaudenzio et al., 2016), which are consistent with the reactions to a vortex challenge in patients with VU (Boyden et al., 2016; Metzger et al., 1976) and are in contrast to the more sustained calcium responses mediated by IgE receptor stimulation (Supplementary Figure S2d) that results in compound exocytosis and slower but stronger and more prolonged reactions in mice than those produced by GPCRs (Gaudenzio et al., 2016).

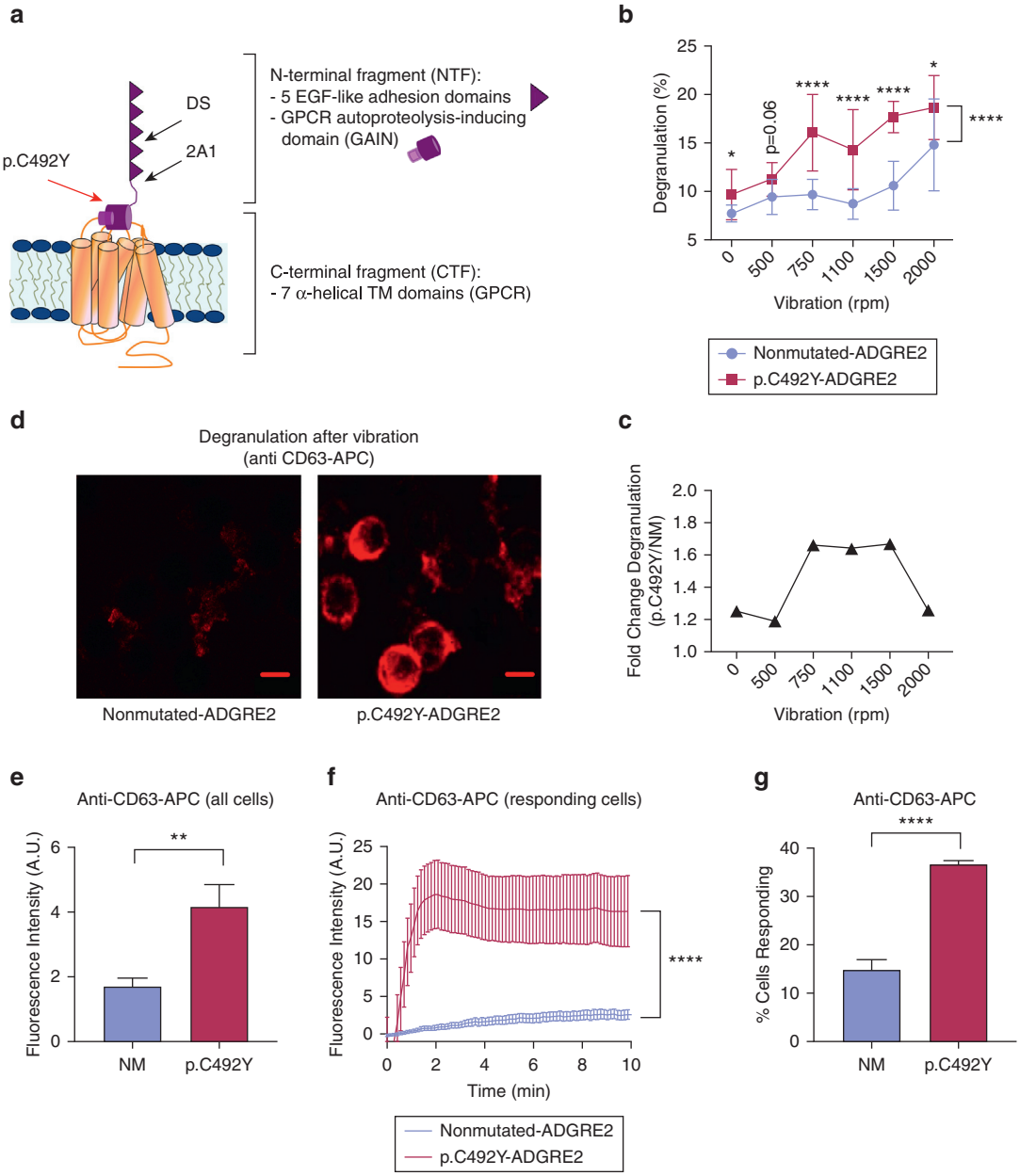

Figure 1. Characterization of vibration-induced degranulation. (**a**) Depiction of ADGRE2. The NTF and CTF, translated as a single polypeptide and self-cleaved in the GAIN domain in the endoplasmic reticulum, remain noncovalently linked (Kwakkenbos et al., 2002). Arrows indicate the location of p.C492Y and binding sites for DS and the 2A1 antibody. (**b**) β-Hexosaminidase release induced by vibration (20 minutes) in NM-ADGRE2 or p.C492Y-ADGRE2 cells. Data are mean ± SD. Student *t*-test was used for the point-by-point comparisons and a two-way ANOVA for comparison between the curves (side bracket). (**c**) Fold changes in degranulation (from data in **b**). (**d**) Images of CD63 surface expression 5 minutes after vibration (750 r.p.m.). Bar = 10 μm. (**e**) Anti–CD63-APC fluorescent intensity 10 minutes after vibration; (n ≥ 77). (**f**) Anti–CD63-APC intensity after vibration in responsive cells; (n = 10). (**g**) Percentage of responsive cells. Data are mean ± SEM in **e**–**g**. $*P < 0.05$; $**P < 0.005$; $****P < 0.0001$. APC, allophycocyanin; AU, arbitrary units; CTF, C-terminal fragment; DS, dermatan sulfate; NM, nonmutated; NTF, N-terminal fragment.

Similar to the populational analysis, confocal single-cell measurements using Fluo-8, which readily detected calcium elevations with the expected kinetics after stimulation of the IgE receptor or thapsigargin treatment in LAD2 cells (Supplementary Figure S2d and e) (Suzuki et al., 2014), showed enhanced calcium responses to vibration in cells with p.C492Y-ADGRE2 (Figure 2b–d), and this increase was abolished in calcium free media (Figure 2c). Because ligation of ADGRE2 by 2A1 activates PLC-β in monocytic cells (I et al., 2017) and PLC activity leads to calcium release through the production of IP3, we explored the involvement of this pathway in the calcium responses. Unlike an inactive structural analog (U73343), inhibition of PLC by U73122 or inhibition of IP3 channels by 2-aminoethoxydiphenyl borate (2APB) blunted the calcium responses in p.C492Y-ADGRE2 cells (Figure 2c and d). Our data thus implicate PLC and mobilization of intracellular calcium in the transients induced by vibration. A contribution of extracellular calcium influx cannot be excluded because 2-aminoethoxydiphenyl borate is also an inhibitor of store operating calcium

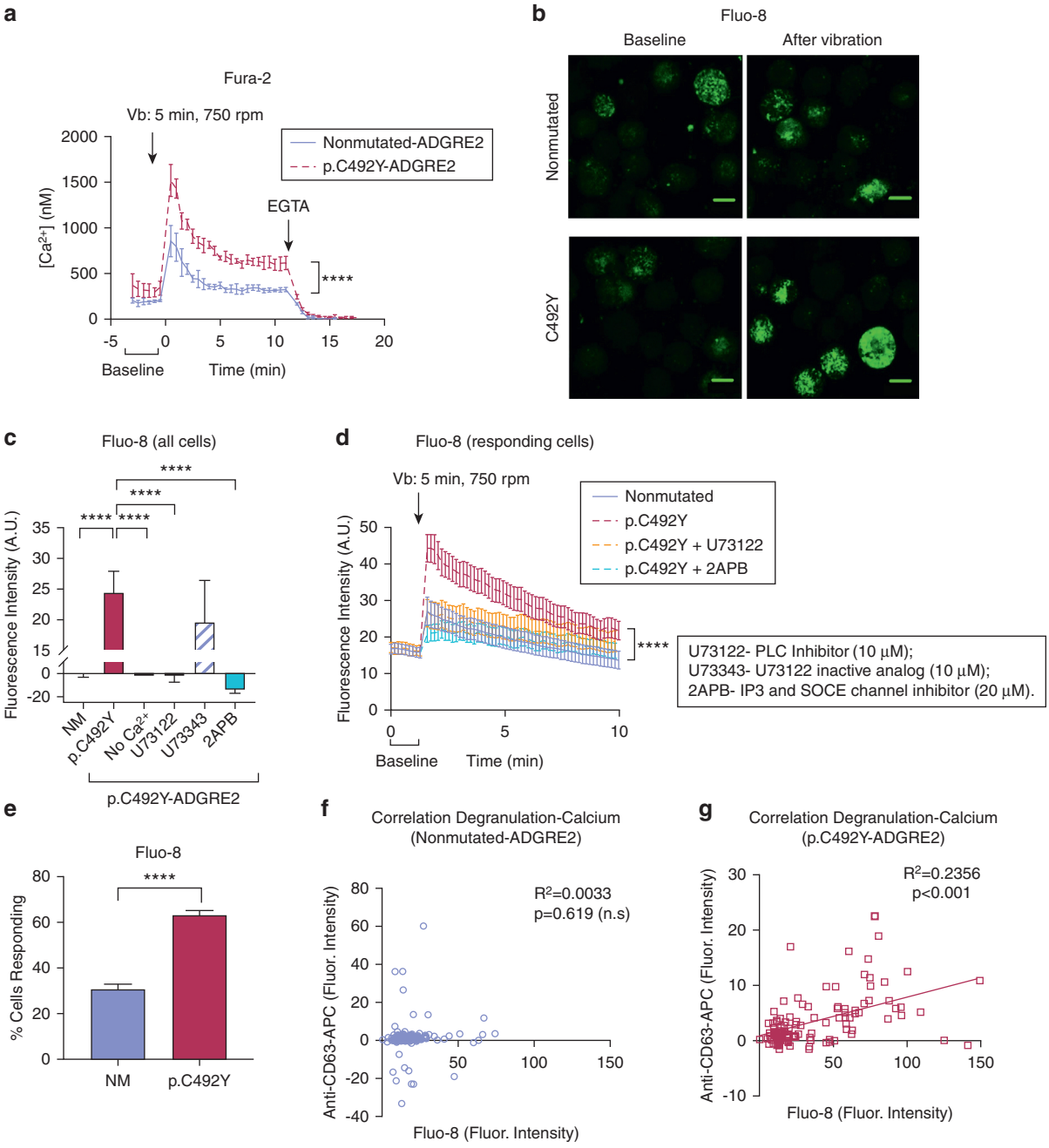

Figure 2. Vibration causes transient calcium mobilization. (**a**) Changes in intracellular calcium measured by Fura-2 in NM-ADGRE2 or p.C492Y-ADGRE2 cells. Data are mean ± SD of two experiments performed in triplicate. (**b**) Images of changes in intracellular calcium after Vb using Fluo-8. Scale Bar = 10 µm. (**c, d**) Average Fluo-8 fluorescence intensity of **(c)** all cells 5 minutes after Vb or **(d)** in responding cells (with signals above baseline) overtime, with or without extracellular calcium and in cells pretreated with inhibitors, as indicated. Data are mean ± SEM (n ≥ 19). (**e**) Percentage of responsive cells. Data are mean ± SEM (n ≥ 77 cells). (**f, g**) Pearson correlation between calcium changes (Fluo-8 intensity) and degranulation (anti−CD63-APC intensity) from n = 4 experiments normalized to average intensities. ***$P < 0.0001$. Two-way ANOVA was used in **a** and **d**. APC, allophycocyanine; AU, arbitrary units; NM, nonmutated; PLC, phospholipase C; SOCE, store operating calcium channels; Vb, vibration.

channels and, to a degree, an inhibitor of transient receptor potential isoforms (Bootman et al., 2002).

As in degranulation, the expression of p.C492Y-ADGRE2 increased both the magnitude of the calcium responses per cell basis (i.e., in cells with intensities above baseline after vibration) (Figure 2d) and the number of cells with positive responses to vibration (Figure 2e). Only in cells expressing p.C492Y-ADGRE2 did maximal Fluo-8 intensity correlate with the extent of degranulation after vibration at 750 r.p.m. (Figure 2f and g), consistent with the conclusion that vibration normally causes calcium fluxes through ADGRE2 that translate into limited or no degranulation, but both processes are enhanced and linked when the p.C492Y variant is present.

Even though calcium is essential for mast cell degranulation, the strength and duration of calcium changes can

determine the overall functional consequences. For instance, activation of the IgE receptor by low-affinity antigens induces lower calcium responses and does not render important degranulation as high-affinity antigens do. However, they transmit different sets of signals with distinct functional outcomes (Suzuki et al., 2014). Overall, the observations support the concept that the structure of ADGRE2 allows mast cells to discriminate the strength of mechanical stimulation and tune the responses accordingly as vibration triggers calcium responses even in cells with the normal variant. Such discrimination of the mechanical strength may be of importance for the immunomodulatory functions of mast cells, much like has been reported for the concentration (Gonzalez-Espinosa et al., 2003) or affinity of antigens (Suzuki et al., 2014) in IgE receptor-mediated activation. However, the molecular and physiological basis for this tuning of the responses and the relevant type of physiological physical stimulus need further investigation. For instance, polymerization of extracellular matrix components, which occurs during wound healing, may constitute a mechanical stimulus for aGPCRs in vivo, as reported by Petersen et al. (2015) or the crawling of skin parasites that can bind skin glycosaminoglycans (Merida-de-Barros et al., 2018) could mimic a vibration stimulus (stretching or treading). It is tempting to speculate that various physical forces may cause limited but advantageous mast cell responses for the host (i.e., recruitment of immune cells, regulation of wound healing, induction of one or both, itch and pain sensing, etc.) without causing a full mast cell response that could be damaging.

Vibration of mast cells with p.C492Y-ADGRE2 induces activation of ERK1/2 and PI3K

We next investigated whether other signaling pathways are activated by vibration. Similar to GPCRs and unlike IgE receptor-mediated activation (Kuehn and Gilfillan, 2007; Mócsai et al., 2003), vibration did not elicit detectable phosphorylation of Src kinases or spleen tyrosine kinase (Supplementary Figure S3a) in p.C492Y-ADGRE2 mast cells. However, vibration prominently increased pathways often associated with agonist-stimulated GPCRs (Gilfillan and Tkaczyk, 2006), such as phosphorylation of protein kinase B (AKT) (Figure 3a and Supplementary Figure S3b), known to be activated in a PI3K-dependent manner (Manning and Toker, 2017) and phosphorylation of ERK1/2 (Figure 3b and Supplementary Figure S3c). However, other MAPK pathways, including c-Jun N-terminal kinase and p38 (Figure 3b), were not activated. The extent of AKT and ERK1/2 phosphorylation induced by vibration was robust and comparable to that induced by activation of mast cells through the IgE receptor (Supplementary Figure S3d).

PKC stimulation occurs downstream of PLC activation. Since PKC can mediate PI3K (Kawakami et al., 2004; Ziemba and Falke, 2018) or MAPK/ERK kinase (MEK)/ERK1/2 pathway activation (Mendoza et al., 2011), we examined its involvement in the regulation of these pathways. Pretreatment with a pan-PKC inhibitor, Gö6983, somewhat reduced AKT phosphorylation induced by vibration, albeit the differences did not reach statistical significance (Figure 3c) and did not affect ERK1/2 (Figure 3d) phosphorylation, suggesting that PI3K and EK1/2 pathways are activated by mechanisms largely independent of PKC.

We also examined the potential cross-interactions between PI3K and ERK1/2 pathways. Inhibition of MEK/ERK1/2 did not prevent vibration-induced phosphorylation of AKT (Figure 3c) but blunted ERK1/2 phosphorylation (Figure 3d). In contrast, the pan-inhibitor of PI3K, wortmannin, markedly diminished AKT activation (Figure 3c) and ERK1/2 phosphorylation (Figure 3d). LY294002, a less potent PI3K inhibitor, only partially reduced ERK1/2 phosphorylation (Figure 3d). Although we cannot exclude potential off-target effects of wortmannin, the results suggest a directional crosstalk between these pathways where activation of PI3K contributes to ERK1/2 activation but not vice versa.

PLC activation and calcium mobilization are critical for both PI3K and ERK1/2 activation

We then examined the involvement of PLC stimulation on vibration-induced PI3K and ERK1/2 phosphorylation. An inhibitor of PLC blocked both AKT (Figure 4a) and ERK1/2 (Figure 4b) phosphorylation, while a structural analog of this inhibitor did not. Blockade of calcium fluxes, but not inhibition of PKC, obliterated ERK1/2 and AKT phosphorylation (Figure 4a and b), suggesting that activation of PLC by vibration and consequent calcium mobilization are required for both PI3K and ERK1/2 activation. Given that PI3K may also regulate ERK1/2 phosphorylation (Figure 3d), calcium could activate ERK1/2 partly through PI3K-dependent pathways. Other points of interaction upstream the molecules affected by those inhibitors are possible because MEK/ERK1/2 and PI3K/Akt signaling cascades crosstalk in multiple points (Mendoza et al., 2011) (see summary in Figure 6d).

A similar chain of events for ADGRE2 activation was reported in human monocytic cell lines by crosslinking ADGRE2 with immobilized 2A1 antibody (I et al., 2017) in the absence of mechanical forces. Although it is unclear why crosslinking of ADGRE2 would activate monocytic cells in static conditions whereas in mast cells vibration is required, both studies reinforce the notion of a consensus chain of signaling events elicited by ADGRE2 activation that are initiated by PLC activation and calcium fluxes, followed by PI3K and MAPK cascades, which in the case of mechanically stimulated mast cells, were restricted to ERK1/2.

Initiation of GPCR signaling involves heterotrimeric G-proteins, although in aGPCRs, the specific subtypes have not been well-characterized (Hamann et al., 2015). Activation of PLC usually depends on $\beta\gamma$, α_q, or α_{11} G-subunits (Boyer et al., 1994). Inhibition of $\beta\gamma$ by gallein, α_q and α_{11} subunits by YM254890, or $\alpha_{i/o}$ subunits by pertussis toxin (PTX) did not significantly prevent the activation of AKT or ERK1/2 (Figure 4c and d). However, the same concentrations of PTX and YM254890 were effective in reducing MRGPRX2-mediated degranulation (Supplementary Figure S4) (Subramanian et al., 2013). Thus, PLC-dependent activation of PI3K and ERK pathways induced by vibration is independent of these subunits, although involvement of other α subtypes, such as α_{16}, is possible, as reported (I et al., 2017).

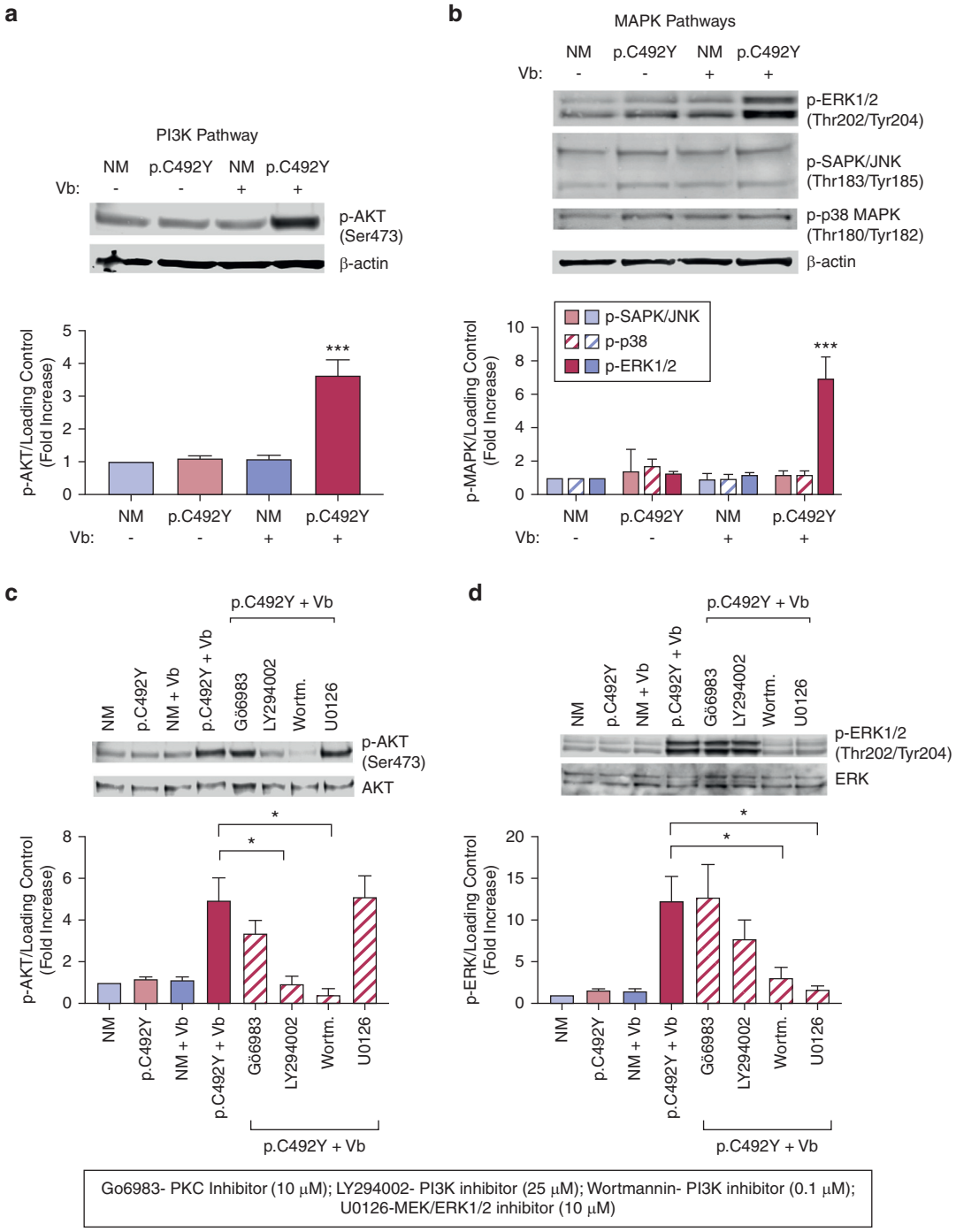

Figure 3. Activation of PI3K and ERK1/2 signaling pathways and their potential crosstalk by mechanoactivation in mast cells with p.C492Y-ADGRE2. DS-bound cells expressing NM-ADGRE2 or p.C492Y-ADGRE2 were lysed after Vb for 5 minutes at 750 r.p.m. (**a, b**) Phosphorylation of (**a**) AKT and (**b**) ERK1/2, SAPK/JNK, and p38. (**c, d**) Effects of inhibition of PKC, PI3K, and MEK1/2 on (**c**) AKT and (**d**) ERK1/2 phosphorylation. Inhibitors were added 20 minutes before Vb. The histograms in **a–d** show the quantification of band intensities (normalized by total AKT/ERK1/2 protein or β-actin) from n > 3 experiments and expressed as fold change compared with nonvibrated NM-ADGRE2–expressing cells. Data are mean ± SEM. *$P < 0.05$; ***$P \leq 0.0001$. AKT, protein kinase B; DS, dermatan sulfate; ERK, extracellular signal–regulated kinase; JNK, c-Jun N-terminal kinase; MEK, MAPK/ERK kinase; NM, nonmutated; PI3K, phosphoinositide 3-kinase; SAPK, stress-activated protein kinase; Vb, vibration.

Signaling requirements for vibration-induced mast cell responses

Because of the potential implications in patients with VU, we next investigated which signaling pathways are required for vibration-induced degranulation. Using confocal imaging of CD63 externalization (Figure 5a and b) or β-hexosaminidase release (Figure 5c) in the presence of various inhibitors, we determined that PLC activation and consequent calcium mobilization and PKC activation are all necessary for degranulation. Furthermore, downstream of PLC and calcium, PI3K pathways only partly contributed to degranulation (Figure 5b and c), whereas ERK1/2 was dispensable

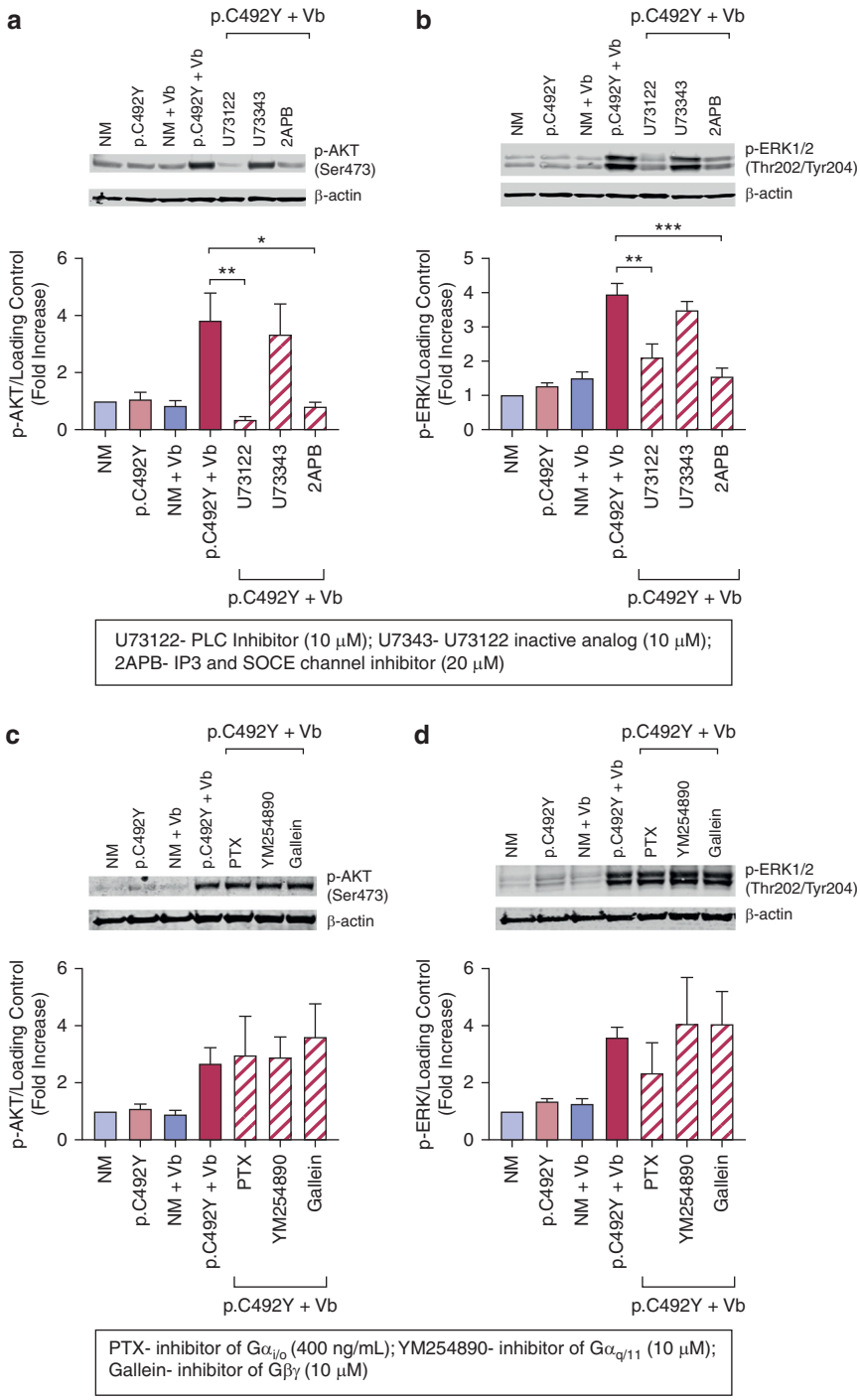

Figure 4. PLC activation and calcium mobilization are critical for PI3K and ERK1/2 activation independently of βγ, $\alpha_{q/11/14}$, and $\alpha_{i/o}$ G-protein subunits. Effects of (**a** and **b**) inhibitors for PLC, IP3, and SOCE channels or (**c** and **d**) inhibitors of G-protein subunits βγ, $\alpha_{i/o}$, and $\alpha_{q/11}$, as indicated on vibration-induced (**a, c**) AKT and (**b, d**) ERK1/2 phosphorylation. DS-attached LAD2 cells expressing NM-ADGRE2 or p.C492Y-ADGRE2 were treated with inhibitors for 20 minutes and vibrated for 5 minutes at 750 r.p.m. Histograms represent band intensities (normalized by total AKT, ERK1/2 protein or β-actin) from $n > 3$ experiments and calculated as fold change compared with nonvibrated, NM-ADGRE2–expressing cells. Data are mean ± SEM. $^*P < 0.05$; $^{**}P < 0.01$; $^{***}P < 0.001$. AKT, protein kinase B; DS, dermatan sulfate; ERK, extracellular signal–regulated kinase; LAD2, laboratory of allergic diseases-2 human mast cell line; NM, nonmutated; PLC, phospholipase C; PI3K, phosphoinositide 3-kinase; SOCE, store operating calcium channels; Vb, vibration.

(Figure 5a–c). Degranulation was also blocked by PTX (Figure 5c), although AKT and ERK1/2 signaling was PTX-independent (Figure 4c and d), suggesting that degranulation depends on both $\alpha_{i/o}$-sensitive and -insensitive pathways (Figure 6d). The specific nature of the $\alpha_{i/o}$ (PTX)-mediated events, as for other GPCRs in mast cells (Subramanian et al., 2013), remains to be elucidated.

Because vibration prominently activated ERK1/2 but had no role in degranulation, we interrogated its involvement in other mast cell responses, particularly PGD_2 release. PGD_2 is one of the most abundant eicosanoid products formed by mast cells as an early de novo mediator (Gilfillan and Tkaczyk, 2006), and ERK1/2 is required for its production through activation of phospholipase A2 (Kuehn et al., 2008). Indeed, vibration-induced PGD_2 release, particularly in cells with p.C492Y-ADGRE2, was blunted by MEK/ERK1/2 inhibition (Figure 6a). In addition, calcium mobilization and PKC were key to this response, with a partial contribution of PI3K (Figure 6a and b). Blockade of $\alpha_{i/o}$, but not α_q, slightly reduced PGD_2 release, suggesting a contributory role of $\alpha_{i/o}$-dependent signals. However, PGD_2 release induced by vibration was especially dependent on PLC-dependent

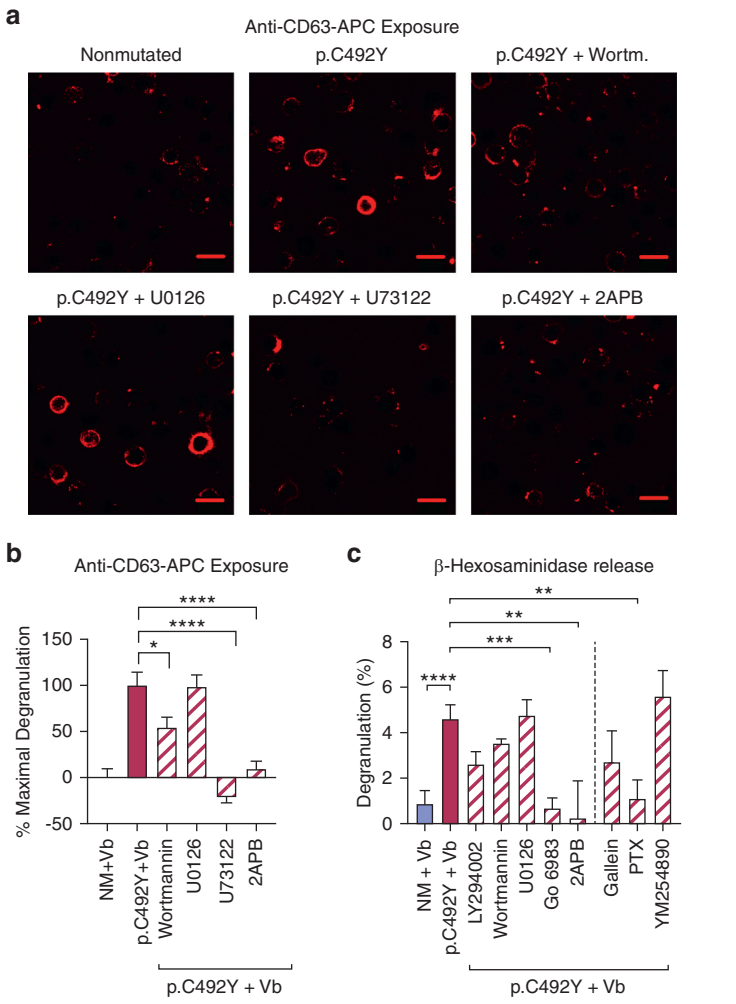

U0126-MEK/ERK1/2 inhibitor (10 μM); U73122-PLC Inhibitor (10 μM); 2APB-IP3 and SOCE channel inhibitor (20 μM); Go6983- PKC Inhibitor (10 μM); LY294002-PI3K inhibitor (25 μM); Wortmannin- PI3K inhibitor (0.1 μM); Gallein-Gβγ inhibitor (10 μM); PTX- $G\alpha_{i/o}$ inhibitor (400 ng/mL); YM254890- $G\alpha_{q/11}$ inhibitor (10 μM)

Figure 5. PLC and calcium and PKC axis, and PTX-sensitive pathways are critical for vibration-induced degranulation, whereas MEK/ERK1/2 is dispensable. LAD2 cells expressing NM-ADGRE2 or p.C492Y-ADGRE2 plated on DS-coated dishes were treated with the indicated inhibitors for 20 minutes before Vb. (**a**) Representative confocal images of anti−CD63-APC on the membrane after vibration for 5 minutes. Bar = 20 μm. (**b**) Quantification of degranulation from data shown in **a**. Fluorescent intensity of anti−CD63-APC in individual cells (n > 264 cells) was determined and expressed as percentage decrement (Δ) of the maximal response (i.e., fluorescent intensity of cells expressing p.C492Y-ADGRE2), being the minimal response fluorescent intensity of anti−CD63-APC in cells with NM-ADGRE2. **(c)** β-Hexosaminidase release after 20 minutes vibration. Data are mean ± SEM, n ≥ 12. $^*P < 0.05$; $^{**}P < 0.005$; $^{***}P < 0.001$; $^{****}P < 0.0001$. APC, allophycocyanin; DS, dermatan sulfate; ERK, extracellular signal −regulated kinase; LAD2, laboratory of allergic diseases-2 human mast cell line; NM, nonmutated; PKC, protein kinase C; PLC, phospholipase C; PI3K, phosphoinositide 3-kinase; PTX, pertussis toxin; SOCE, store operating calcium channels; Vb, vibration.

pathways, highlighting the key role for PLC and downstream signals in mechanoactivation of mast cells.

PGD2, an unrecognized mediator in VU

Mirroring the increase in PGD_2 production by mast cells after vibration in vitro, we found that in patients with VU, unlike normal subjects, PGD_2 was elevated in the venous return of the arm early after vibration. PGD_2 remained elevated over baseline 30 minutes after vortex challenge (Figure 6c). Although confirmation in larger cohorts is needed, the findings suggest a potential role of PGD_2 in the pathology of VU. PGD_2 can mediate immediate hypersensitivity processes causing hypotension and flushing, but it can also play anti-inflammatory roles (Boyce, 2007; Kulinski et al., 2016) and reduce vascular permeability by tightening the endothelial barrier (Nakamura et al., 2016). Because the increase in PGD_2 levels seemed to be sustained longer (Figure 6c) than those of histamine (Boyden et al., 2016; Epstein and Kidd, 1981; Ting et al., 1983), one hypothesis would be that PGD_2 downregulates the responses to vibration, contributing to the transient nature of VU pathology. It would be of interest to determine whether PGD_2 is not generated in patients with vibratory angioedema (Keahey et al., 1987), who unlike those with in VU, have long-lasting responses.

Concluding remarks

Herein, we have identified the signaling pathways activated by physical forces in mast cells expressing p.C492Y-ADGRE2, a variant associated with familial VU that renders skin mast cells more susceptible to friction (Boyden et al., 2016). Mechanical signaling encompasses PLC activation as a key early step for mast cell degranulation and PGD_2 release and a parallel PTX-sensitive pathway, also essential for degranulation. The requirement for PLC resonates with the reported gain of PLCγ2 function in a form of inherited cold urticaria where mast cells are also key (Ombrello et al., 2012). Thus, exploration of the role of distinct PLC isoforms and PLC-derived signals in other physical urticarias may be of interest. Downstream of PLC, PKC and calcium were critical for vibration-induced degranulation and eicosanoid production, whereas ERK1/2 was only required for PGD_2 release. The distinct requirement for these signals on degranulation

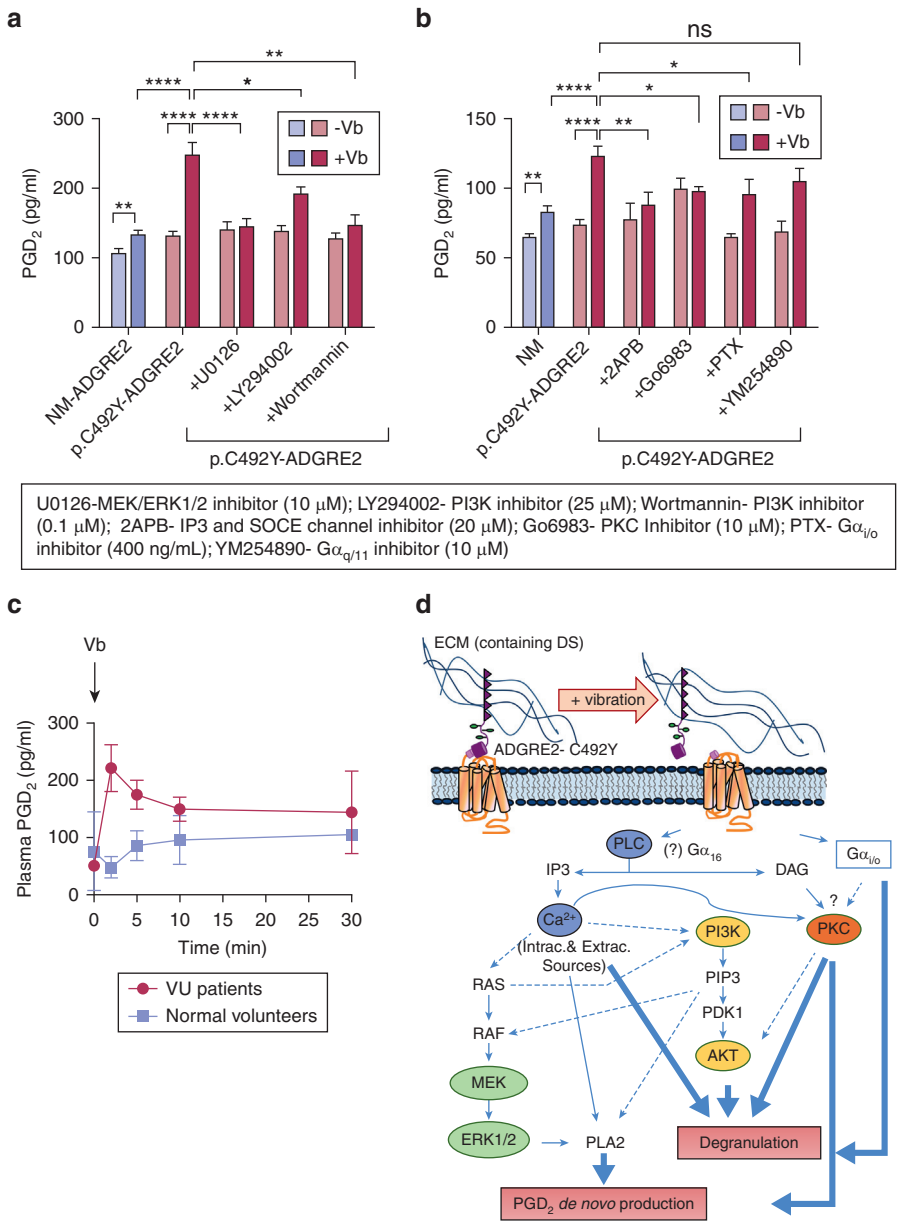

Figure 6. Vibration-induced PGD_2 release is dependent on PLC and calcium, PKC, and MEK/ERK1/2 and vortex challenge in patients with VU increases serum PGD_2. (**a, b**) PGD_2 release induced by vibration in mast cells expressing NM-ADGRE2 or p.C492Y-ADGRE2 in the presence or absence of the indicated inhibitors. PGD_2 was measured in the supernatants of cells vibrated or not at 750 r.p.m. for 10 minutes. Data are mean ± SEM; $n \geq 9$. $^*P < 0.05$; $^{**}P < 0.005$; $^{****}P < 0.0001$. (**c**) PGD_2 in the serum of two patients with VU and two control subjects after a vibratory challenge. (**d**) Representation of the proposed signaling pathways involved in mechanical activation of mast cells. Doted lines are potential ways of crosstalk on the basis of our data or the literature (Cullen and Lockyer, 2002; Danciu et al., 2003; Mendoza et al., 2011; Yano et al., 1998). APC, allophycocyanine; DS, dermatan sulfate; ECM, extracellular matrix; ERK, extracellular signal—regulated kinase; MEK, MAPK/ERK kinase; NM, nonmutated; ns, not significant; PGD_2, prostaglandin G_2; PKC, protein kinase C; PLC, phospholipase C; PI3K, phosphoinositide 3-kinase; PTX, pertussis toxin; SOCE, store operating calcium channels; Vb, vibration; VU, vibratory urticaria.

and PGD_2 release are generally consistent with their roles in IgE receptor or GPCR activation (Gilfillan and Tkaczyk, 2006; Kimata et al., 2000; Xing et al., 1997), although their cross-talk appears to be distinct for ADGRE2 (Figure 6d). Our findings not only add to the knowledge of the enigmatic signaling events initiated by mechanical stimulation, their hierarchy and cross-interaction, but also may help design novel therapeutic approaches for VU and give clues into mechanisms for other physical urticarias.

MATERIALS AND METHODS

Further details on the experimental procedures can be found in Supplementary Methods.

Patients

Patients with VU were enrolled and evaluated at the National Institute of Health Clinical Center under a protocol approved by the Institutional Review Board of the National Institute of Allergy and Infectious Diseases (09-I-0126). All subjects provided written informed consent. VU symptoms in a clinical setting were elicited as described (Boyden et al., 2016).

Cell activation

LAD2 cells (Kirshenbaum et al., 2003) transfected with the *ADGRE2* constructs by nucleofection (Cruse et al., 2013) were plated overnight on wells coated with 100 μg/ml DS (chondroitin sulfate B, Sigma-Aldrich, St. Louis, MO). After gentle washing, cells were resuspended in 100 μl of prewarmed 4-(2-hydroxyethyl)-1-piperazineethanesulfonic acid (HEPES) buffer and vibrated at 750 r.p.m. (or as indicated) for 5–20 minutes on an orbital shaker (Eppendorf ThermoMixer C, Eppendorf, Hauppauge, NY) at 37 °C. In some experiments, cells were treated with the indicated concentrations of inhibitors or vehicle (0.1% DMSO) 20 minutes before and during vibration.

Mast cell mediators and signaling

Degranulation was determined as the percentage of β-hexosaminidase released into the media (Kuehn et al., 2010) 20 minutes after vibration. Alternatively, cells plated in DS-coated imaging chambers (Ibidi, Fitchburg, WI #80826) were vibrated for 5 minutes and anti−CD63-allophycocyanin was added (1:20). Confocal images were acquired over time using a Leica TCS SP8 microscope (Leica Microsystems, Buffalo Grove, IL) and processed using Fiji-ImageJ (Schindelin et al., 2012), selecting Region of Interest Manager to determine anti−CD63-allophycocyanin mean fluorescent intensity per cell.

PGD_2 in cell-free supernatants or serum samples was determined by competitive ELISA (Cayman Chemicals, Ann Arbor, MI). Phosphorylation of signaling proteins were determined by Western blotting after vibration for 5 minutes as described (Boyden et al., 2016; Tkaczyk et al., 2002).

Calcium flux measurements

Cells attached to DS-coated chambers were loaded or not with 5 μM Fura-2-acetoxymethyl ester (ThermoFisher Scientific, Waltham, MA) or Fluo-8 acetoxymethyl ester (Abcam, Cambridge, MA), washed, and vibrated at 750 r.p.m. for 5 minutes. Measurements of Fura-2 fluorescence were done using a Perkin Elmer Wallac 1420 Victor2 microplate reader (PerkinElmer, Waltham, MA), as described (Cruse et al., 2013; Grynkiewicz et al., 1985), and changes in fluorescence of calcium-bound Fluo-8 by confocal microscopy. Before imaging, anti−CD63-allophycocyanin at 1:20 dilution was added to simultaneously track mast cell degranulation. Mean fluorescent intensity per cell was measured using Region of Interest Manager, and baseline fluorescence was subtracted from each individual cell.

Statistical analysis

Statistical analysis was conducted using GraphPad Prism (GraphPad, San Diego, CA, version 7.01). Unpaired Student's *t*-test was used for most comparisons unless otherwise indicated. A P-value < 0.05 was considered significant. All experiments were done at two independent times or more and performed at least in triplicate.

Data availability statement

The authors declare that all data supporting the findings of this study are available within the manuscript or from the corresponding author upon request.

ORCIDs

Andrea N. Naranjo: http://orcid.org/0000-0002-8552-545X
Geethani Bandara: http://orcid.org/0000-0002-8053-7769
Yun Bai: http://orcid.org/0000-0002-8035-7485
Margery G. Smelkinson: http://orcid.org/0000-0001-7777-5574
Araceli Tobío: http://orcid.org/0000-0002-7445-2507
Hirsh D. Komarow: http://orcid.org/0000-0001-7012-9406
Steven E. Boyden: http://orcid.org/0000-0002-9334-1466
Daniel L. Kastner: http://orcid.org/0000-0001-7188-4550
Dean D. Metcalfe: http://orcid.org/0000-0002-7781-8260
Ana Olivera: http://orcid.org/0000-0002-0128-5461

CONFLICT OF INTEREST

The authors state no conflict of interest.

ACKNOWLEDGMENTS

This work was supported by the Division of Intramural Research within the National Institute of Allergy and Infectious Diseases and the National Human Genome Research Institute at the National Institutes of Health.

The authors thank the valuable experimental and intellectual contributions of Michael A. Beaven, who unfortunately passed away before the completion of this work. The authors also thank Avanti Desai for valuable technical assistance.

AUTHOR CONTRIBUTIONS

Conceptualization: ANN, AO, DDM; Data Curation: ANN; Formal Analysis: ANN, GB, YB, AO; Funding Acquisition: DLK, DDM; Investigation: ANN, GB; Methodology: ANN, GB, YB, MGS, AT, SEB; Resources: HDK, SEB; Supervision: AO; Visualization: ANN, AO; Writing - Original Draft Preparation: ANN, AO; Writing - Review and Editing: ANN, GB, YB, MGS, AT, HDK, SEB, DLK, DDM, AO

SUPPLEMENTARY MATERIAL

Supplementary material is linked to the online version of the paper at www.jidonline.org, and at https://doi.org/10.1016/j.jid.2020.03.936.

REFERENCES

Bootman MD, Collins TJ, Mackenzie L, Roderick HL, Berridge MJ, Peppiatt CM. 2-aminoethoxydiphenyl borate (2-APB) is a reliable blocker of store-operated Ca2+ entry but an inconsistent inhibitor of InsP3-induced Ca2+ release. FASEB J 2002;16:1145−50.

Boyce JA. Mast cells and eicosanoid mediators: a system of reciprocal paracrine and autocrine regulation. Immunol Rev 2007;217:168−85.

Boyden SE, Desai A, Cruse G, Young ML, Bolan HC, Scott LM, et al. Vibratory urticaria associated with a missense variant in ADGRE2. N Engl J Med 2016;374:656−63.

Boyer JL, Graber SG, Waldo GL, Harden TK, Garrison JC. Selective activation of phospholipase C by recombinant G-protein alpha- and beta gamma-subunits. J Biol Chem 1994;269:2814−9.

Chen TY, Hwang TL, Lin CY, Lin TN, Lai HY, Tsai WP, et al. EMR2 receptor ligation modulates cytokine secretion profiles and cell survival of lipopolysaccharide-treated neutrophils. Chang Gung Med J 2011;34:468−77.

Clapham DE. TRP channels as cellular sensors. Nature 2003;426:517−24.

Cruse G, Beaven MA, Ashmole I, Bradding P, Gilfillan AM, Metcalfe DD. A truncated splice-variant of the FcεRIβ receptor subunit is critical for microtubule formation and degranulation in mast cells. Immunity 2013;38:906−17.

Cullen PJ, Lockyer PJ. Integration of calcium and Ras signalling. Nat Rev Mol Cell Biol 2002;3:339−48.

Danciu TE, Adam RM, Naruse K, Freeman MR, Hauschka PV. Calcium regulates the PI3K-Akt pathway in stretched osteoblasts. FEBS Lett 2003;536:193−7.

Epstein PA, Kidd KK. Dermo-distortive urticaria: an autosomal dominant dermatologic disorder. Am J Med Genet 1981;9:307−15.

Gaudenzio N, Sibilano R, Marichal T, Starkl P, Reber LL, Cenac N, et al. Different activation signals induce distinct mast cell degranulation strategies. J Clin Invest 2016;126:3981−98.

Gilfillan AM, Tkaczyk C. Integrated signalling pathways for mast-cell activation. Nat Rev Immunol 2006;6:218−30.

Gonzalez-Espinosa C, Odom S, Olivera A, Hobson JP, Martinez ME, Oliveira-Dos-Santos A, et al. Preferential signaling and induction of allergy-promoting lymphokines upon weak stimulation of the high affinity IgE receptor on mast cells. J Exp Med 2003;197:1453−65.

Grynkiewicz G, Poenie M, Tsien RY. A new generation of Ca2+ indicators with greatly improved fluorescence properties. J Biol Chem 1985;260:3440−50.

Hamann J, Aust G, Araç D, Engel FB, Formstone C, Fredriksson R, et al. International union of basic and clinical pharmacology. XCIV. Adhesion G protein-coupled receptors. Pharmacol Rev 2015;67:338−67.

Huang YS, Chiang NY, Hu CH, Hsiao CC, Cheng KF, Tsai WP, et al. Activation of myeloid cell-specific adhesion class G protein-coupled receptor EMR2 via ligation-induced translocation and interaction of receptor subunits in lipid raft microdomains. Mol Cell Biol 2012;32:1408−20.

I K-Y, Huang Y-S, Hu C-H, Tseng W-Y, Cheng C-H, Stacey M, et al. Activation of adhesion GPCR EMR2/ADGRE2 induces macrophage differentiation and inflammatory responses via Gα16/Akt/MAPK/NF-κB signaling pathways. Front Immunol 2017;8:373.

Karpus ON, Veninga H, Hoek RM, Flierman D, van Buul JD, Vandenakker CC, et al. Shear stress-dependent downregulation of the adhesion-G protein-coupled receptor CD97 on circulating leukocytes upon contact with its ligand CD55. J Immunol 2013;190:3740−8.

Kawakami Y, Nishimoto H, Kitaura J, Maeda-Yamamoto M, Kato RM, Littman DR, et al. Protein kinase C betaII regulates Akt phosphorylation on Ser-473 in a cell type- and stimulus-specific fashion. J Biol Chem 2004;279:47720−5.

Keahey TM, Indrisano J, Lavker RM, Kaliner MA. Delayed vibratory angioedema: insights into pathophysiologic mechanisms. J Allergy Clin Immunol 1987;80:831–8.

Kimata M, Inagaki N, Kato T, Miura T, Serizawa I, Nagai H. Roles of mitogen-activated protein kinase pathways for mediator release from human cultured mast cells. Biochem Pharmacol 2000;60:589–94.

Kirshenbaum AS, Akin C, Wu Y, Rottem M, Goff JP, Beaven MA, et al. Characterization of novel stem cell factor responsive human mast cell lines LAD 1 and 2 established from a patient with mast cell sarcoma/leukemia; activation following aggregation of FcεRI or FcγRI. Leuk Res 2003;27:677–82.

Kuehn HS, Gilfillan AM. G protein-coupled receptors and the modification of FcεRI-mediated mast cell activation. Immunol Lett 2007;113:59–69.

Kuehn HS, Radinger M, Gilfillan AM. Measuring mast cell mediator release. Curr Protoc Immunol 2010;91:7.38.1–7.38.9.

Kuehn HS, Swindle EJ, Kim MS, Beaven MA, Metcalfe DD, Gilfillan AM. The phosphoinositide 3-kinase-dependent activation of Btk is required for optimal eicosanoid production and generation of reactive oxygen species in antigen-stimulated mast cells. J Immunol 2008;181:7706–12.

Kulinski JM, Muñoz-Cano R, Olivera A. Sphingosine-1-phosphate and other lipid mediators generated by mast cells as critical players in allergy and mast cell function. Eur J Pharmacol 2016;778:56–67.

Kwakkenbos MJ, Chang GW, Lin HH, Pouwels W, de Jong EC, van Lier RAW, et al. The human EGF-TM7 family member EMR2 is a heterodimeric receptor expressed on myeloid cells. J Leukoc Biol 2002;71:854–62.

Langenhan T, Aust G, Hamann J. Sticky signaling–adhesion class G protein-coupled receptors take the stage. Sci Signal 2013;6:re3.

Le QT, Lyons JJ, Naranjo AN, Olivera A, Lazarus RA, Metcalfe DD, et al. Impact of naturally forming human α/β-tryptase heterotetramers in the pathogenesis of hereditary α-tryptasemia. J Exp Med 2019;216:2348–61.

Manning BD, Toker A. AKT/PKB signaling: navigating the network. Cell 2017;169:381–405.

Mendoza MC, Er EE Jr, Blenis J. The Ras-ERK and PI3K-mTOR pathways: cross-talk and compensation. Trends Biochem Sci 2011;36:320–8.

Merida-de-Barros DA, Chaves SP, Belmiro CLR, Wanderley JLM. Leishmaniasis and glycosaminoglycans: a future therapeutic strategy? Parasit Vectors 2018;11:536.

Metzger WJ, Kaplan AP, Beaven MA, Irons JS, Patterson R. Hereditary vibratory angioedema: confirmation of histamine release in a type of physical hypersensitivity. J Allergy Clin Immunol 1976;57:605–8.

Mócsai A, Zhang H, Jakus Z, Kitaura J, Kawakami T, Lowell CA. G-protein-coupled receptor signaling in Syk-deficient neutrophils and mast cells. Blood 2003;101:4155–63.

Nakamura T, Fukaya T, Uto T, Takagi H, Arimura K, Tono T, et al. Selective depletion of basophils ameliorates immunoglobulin E-mediated anaphylaxis. Biochem Biophys Rep 2016;9:29–35.

Ombrello MJ, Remmers EF, Sun G, Freeman AF, Datta S, Torabi-Parizi P, et al. Cold urticaria, immunodeficiency, and autoimmunity related to PLCG2 deletions. N Engl J Med 2012;366:330–8.

Petersen SC, Luo R, Liebscher I, Giera S, Jeong SJ, Mogha A, et al. The adhesion GPCR GPR126 has distinct, domain-dependent functions in Schwann cell development mediated by interaction with laminin-211. Neuron 2015;85:755–69.

Purcell RH, Hall RA. Adhesion G protein-coupled receptors as drug targets. Annu Rev Pharmacol Toxicol 2018;58:429–49.

Schindelin J, Arganda-Carreras I, Frise E, Kaynig V, Longair M, Pietzsch T, et al. Fiji: an open-source platform for biological-image analysis. Nat Methods 2012;9:676–82.

Scholz N, Gehring J, Guan C, Ljaschenko D, Fischer R, Lakshmanan V, et al. The adhesion GPCR latrophilin/CIRL shapes mechanosensation. Cell Rep 2015;11:866–74.

Scholz N, Monk KR, Kittel RJ, Langenhan T. Adhesion GPCRs as a putative class of metabotropic mechanosensors. Handb Exp Pharmacol 2016;234:221–47.

Stacey M, Chang GW, Davies JQ, Kwakkenbos MJ, Sanderson RD, Hamann J, et al. The epidermal growth factor-like domains of the human EMR2 receptor mediate cell attachment through chondroitin sulfate glycosaminoglycans. Blood 2003;102:2916–24.

Subramanian H, Gupta K, Lee D, Bayir AK, Ahn H, Ali H. β-Defensins activate human mast cells via mas-related gene X2. J Immunol 2013;191:345–52.

Suzuki R, Leach S, Liu W, Ralston E, Scheffel J, Zhang W, et al. Molecular editing of cellular responses by the high-affinity receptor for IgE. Science 2014;343:1021–5.

Ting S, Reimann BE, Rauls DO, Mansfield LE. Nonfamilial, vibration-induced angioedema. J Allergy Clin Immunol 1983;71:546–51.

Tkaczyk C, Metcalfe DD, Gilfillan AM. Determination of protein phosphorylation in FcεRI-activated human mast cells by immunoblot analysis requires protein extraction under denaturing conditions. J Immunol Methods 2002;268:239–43.

Xing M, Firestein BL, Shen GH, Insel PA. Dual role of protein kinase C in the regulation of cPLA2-mediated arachidonic acid release by P2U receptors in MDCK-D1 cells: involvement of MAP kinase-dependent and -independent pathways. J Clin Invest 1997;99:805–14.

Yano S, Tokumitsu H, Soderling TR. Calcium promotes cell survival through CaM-K kinase activation of the protein-kinase-B pathway. Nature 1998;396:584–7.

Yona S, Lin HH, Dri P, Davies JQ, Hayhoe RPG, Lewis SM, et al. Ligation of the adhesion-GPCR EMR2 regulates human neutrophil function. FASEB J 2008;22:741–51.

Ziemba BP, Falke JJ. A PKC-MARCKS-PI3K regulatory module links Ca2+ and PIP3 signals at the leading edge of polarized macrophages. PLoS One 2018;13:e0196678.

SUPPLEMENTARY MATERIALS AND METHODS

Antibodies and inhibitors

Antibodies against extracellular signal−regulated kinase 1/2, phospho−extracellular signal−regulated kinase 1/2 (Thr202/Tyr204), protein kinase B, phospho−protein kinase B (Ser473), phospho−protein kinase B(Thr308), phospho−stress-activated protein kinase /c-Jun N-terminal kinas (Thr183/Tyr185), and phospho-p38 (Thr180/Tyr182) were purchased from Cell Signaling (Danvers, MA). Anti−β-actin clone AC-15 was from Sigma-Aldrich (St. Louis, MO); IRDye 680RD goat anti−mouse IgG (red) and IRDye 800CW donkey anti-rabbit IgG (green) were from LI-COR Biosciences (Lincoln, NE). Anti−CD63-allophycocyanin was from ThermoFisher Scientific (Waltham, MA) and mouse anti−human CD312 (2A1) was from Bio-Rad (Hercules, CA). Inhibitors for the G-protein βγ subunit (gallein), protein kinase C (Go6983), phosphoinositide 3-kinase (LY294002 and wortmannin), MAPK/extracellular signal−regulated kinase/extracellular signal−regulated kinase 1/2 (U0126), IP3 receptors (2-aminoethoxydiphenyl borate), G-protein receptor coupling (Pertussis toxin), and phospholipase C (U73122) and its inactive analog (U73343) were from Tocris (Minneapolis, MN). A selective inhibitor of G-protein α_q and α_{11} (YM254890) was from Wako Chemicals (Richmond, VA).

Cell culture

Laboratory of allergic diseases 2 (LAD2) cells were cultured in StemPro-34 SFM medium containing StemPro-34 Nutrient Supplement (Life Technologies-ThermoFisher Scientific, Grand Island, NY); L-glutamine (2 mM), penicillin (100 U/ml) and/or streptomycin (100 μg/ml) (GIBCO, Grand Island, NY), and 100 ng/ml recombinant human SCF (R&D systems, Minneapolis, MN), as described (Kirshenbaum et al., 2003).

ADGRE2 constructs and LAD2 transfection

Nonmutated-*ADGRE2* and p.C492Y-*ADGRE2* were inserted into the pENTR/D-TOPO entry vector (Invitrogen-ThermoFisher Scientifc, Carlsbad, CA), and the constructs were subcloned into the C-terminal Emerald Green Fluorescent Protein (EmGFP)-tagged Vivid Colors pcDNA6.2/C-EmGFP DEST Gateway destination vector (Invitrogen) or into the C-terminal V5-tagged pcDNA3.2/V5 DEST Gateway destination vector (Invitrogen) using the Gateway LR Clonase II Enzyme Mix (Invitrogen) (Boyden et al., 2016). LAD2 cells (2×10^6) were transfected by electroporation using the Amaxa Nucleofector II (Lonza, Walkersville, MD). Cells were washed once with PBS, resuspended in 100 μl of Cell Line Kit V solution (Lonza, Walkersville, MD), mixed with 4 μg of the corresponding *ADGRE2* constructs, and electroporated using preprogrammed electrical parameters (U-025). After nucleofection, 1 ml of culture media was added to the cuvette and cells were transferred to a six-well plate containing an additional ml of media. Transfected LAD2 cells were used for experiments within 24 hours, as we have observed that electroporation often caused a slow but progressive decline in cell viability 24 hours after transfection, limiting other possible manipulations, including knockdown experiments. The transfection efficiency was on the average >70% as determined by FACS analysis of GFP positive cells (see Supplementary Figure S1a).

Determination of degranulation by β-hexosaminidase release

Culture 96-flat bottom well plates were coated with 100 μg/ml dermatan sulfate (chondroitin sulfate B) (Sigma-Aldrich, St. Louise, MO) in PBS for 6 hours at 37 °C or overnight at 4 °C and washed with PBS. In some experiments, wells were coated instead with 100 μg/ml chondroitin sulfate A, 0.01% polylysine, or 50 μg/ml 2A1 mAb. Transfected LAD2 cells as described above were immediately plated in culture media (50,000 cells/well) and allowed to attach to the DS-coated dishes overnight. Alternatively, cells were plated on various concentrations of DS, various glycosaminoglycans, or polylysine (as indicated in the corresponding figure) for 3 hours in prewarmed 4-(2-hydroxyethyl)-1-piperazineethanesulfonic acid (HEPES) buffer (pH: 7.4, 10 mM HEPES, 137 mM NaCl, 2.7 mM KCl, 0.4 mM $Na_2HPO_4 \cdot 7H_2O$, 5.6 mM glucose, 1.8 mM $CaCl_2 \cdot 2H_2O$, 1.3 mM $MgSO_4 \cdot 7H2O$). Adhered cells were gently washed twice with prewarmed HEPES buffer. Plates were vibrated in 100 μl of HEPES buffer at 750 r.p.m. for 5−20 minutes on an orbital shaker (ThermoMixer C, Eppendorf, Hauppauge, NY) at 37 °C. After vibration, plates were centrifuged at 450 g for 5 minutes at 4 °C, and the supernatant was collected to determine the content of released β-hexosaminidase. β-Hexosaminidase activity remaining within the cells was also measured, and the percentage of released β-hexosaminidase was determined as described (Kuehn et al., 2010). The complexity of the experimental design is reflected in a coefficient of variation between degranulation experiments of 16−20%. In some experiments, LAD2 cells were stimulated with the ligand of the MRGPRX2, compound 48 of 80 (0.5 μg/ml) (Sigma-Aldrich) in HEPES buffer for 30 minutes, and β-hexosaminidase release was determined as above.

Determination of mast cell degranulation by confocal microscopy

LAD2 cells were electroporated with the *ADGRE2-V5* constructs and plated (200,000 cells per well) overnight in DS-coated μ-slide 8-well imaging chambers (Ibidi, Madison, WI). Cells were vibrated at 750 r.p.m. for 5 minutes on an orbital shaker at 37 °C. Anti−CD63−allophycocianin was added (1:20 dilution) after vibration at the time of image recording. Receptor independent degranulation by 1 μM thapsigargin or IgE receptor activation were used as positive controls. For IgE-mediated stimulation, LAD2 cells were sensitized with 100 ng/ml of biotinylated IgE overnight, washed, and challenged with 100 ng/ml streptavidin. Confocal images were acquired using a Leica TCS SP8 microscope (Leica Microsystems, Buffalo Grove, IL) equipped with a ×63/1.4NA oil immersion objective, hybrid HyD detectors, adaptive focus control, and an environmental chamber set to 37 °C with 5% CO_2. Images were processed using Fiji-ImageJ (version 1.5a). Individual cells were selected using Region of Interest Manager, and allophycocyanin mean fluorescent intensity per cell was recorded overtime. Background mean fluorescence intensity was subtracted from each individual cell, and the signals from all cells with values above background were averaged overtime.

Calcium flux measurements

Transfected LAD2 cells were plated on black 96-flat bottom well plates (CulturPlate-96 Black, PerkinElmer, Boston, MA) coated with 100 μg/ml DS (50,000 cells/well) and incubated overnight in culture media. Fura-2-acetoxymethyl ester (5 μM) (ThermoFisher Scientific, Waltham, MA) was added to cells for 30 minutes. Adhered cells were gently washed twice with HEPES buffer containing 0.04% BSA and 0.3 mM sulfinpyrazone. Plates were vibrated at 750 r.p.m. for 5 minutes at 37 °C. To determine the minimum and maximal fluorescence signals, 50 μM EGTA or 1 μM thapsigargin, respectively, were added. For IgE receptor stimulation, LAD2 cells were sensitized and challenged as described above. Samples were excited at two wavelengths (340 nm and 380 nm) to detect Fura-2 bound and unbound to calcium, and fluorescence emission was measured at 510 nm using a Perkin Elmer Wallac 1420 Victor2 microplate reader. The ratio of the fluorescence readings was calculated after subtracting the fluorescence of the cells that were not loaded with Fura-2-acetoxymethyl ester. Calcium concentration was calculated using the ratio of fluorescence readings (340 nm and 380 nm) at each time point and the minimal and maximal readings as described (Grynkiewicz et al., 1985).

Alternatively, changes in cytosolic calcium were detected in individual cells by fluorescence of calcium-bound Fluo-8 (Abcam, Cambridge, MA) using a confocal microscope. Following transfection, LAD2 cells were plated overnight on 100 μg/ml DS-coated μ-slide eight-well imaging chambers (250,000 cells per well). Cells were then loaded with 5 μM Fluo-8 acetoxymethyl ester for 30 minutes at 37 °C and 5% CO_2. Adhered cells were washed twice with HEPES buffer, and baseline fluorescence was then recorded. Chambers were vibrated at 750 r.p.m. for 5 minutes on an orbital shaker at 37 °C. Before imaging, anti—CD63-allophycocianin at 1:20 dilution was added to simultaneously track mast cell degranulation. Confocal images were acquired using a Leica TCS SP8 microscope (Leica Microsystems). Images were processed as described for the degranulation measurements by confocal microscopy.

Phosphorylation of downstream molecules: Immunoblotting

Cells transfected with the *ADGRE2-GFP* constructs were plated in DS (100 μg/ml)-coated 24-well plates (250,000 cells per well) overnight, washed, and vibrated in 200 μl HEPES buffer at 750 r.p.m. for 5 minutes at 37 °C. LAD2 cells were lysed in two × denaturing sample suffer (Tkaczyk et al., 2002). Samples were boiled and separated by electrophoresis on 4—12% NuPage Bis-Tris gels (ThermoFisher Scientific). Proteins were transferred to nitrocellulose membranes (0.45 μm pore size, ThermoFisher Scientific) and blots were incubated with the primary antibodies (listed above) overnight at 4 °C on a shaker. Bands were detected using infrared-labeled secondary antibodies and imaging of the bands was performed using an Odyssey CLx Infrared Imaging System (LI-COR Biosciences). Quantification of infrared fluorescence was conducted using Image Studio Lite (version 5.2).

Inhibition experiments

When inhibitors were used to determine their effects on mast cell responses or signaling, LAD2 cells were treated with the corresponding inhibitor or vehicle (0.1% DMSO) 20 minutes before vibration and maintained in the media during vibration. The concentrations used were as follows: Gö6983 (10 μM), LY294002 (25 μM), Wortmannin (0.1 μM), U0126 (10 μM), U73122 (10 μM), U73343 (10 μM), 2-aminoethoxydiphenyl borate (20-50 μM), gallein (10 μM), pertussis toxin (400 ng/mL), and YM254890 (10 μM).

Patients and vortex challenge

Patients with vibratory urticaria were enrolled and evaluated at the National Institutes of Health Clinical Center under a protocol approved by the Institutional Review Board of the National Institute of Allergy and Infectious Diseases (09-I-0126), as described (Boyden et al., 2016). All subjects provided written informed consent. To elicit vibratory urticaria symptoms in a clinical setting, the anterior forearm of a subject was placed horizontally on the 3-inch platform of a laboratory vortex for a 4-minute challenge at 2,500 r.p.m. Serial blood draws at baseline and during the 60 minutes post-challenge period were taken for analysis of prostaglandin D_2 by ELISA.

Prostaglandin D_2 measurements

LAD2 cells were plated (50,000 cells/well) on DS-coated 96-well plates overnight, washed, and subjected to vibration in HEPES buffer (750 r.p.m. for 20 minutes), as described above. Cell-free supernatants or serum sample from patients with vibratory urticaria were analyzed for prostaglandin D_2 by competitive enzyme immunoassay (Cayman Chemicals), according to the manufacturer's instructions.

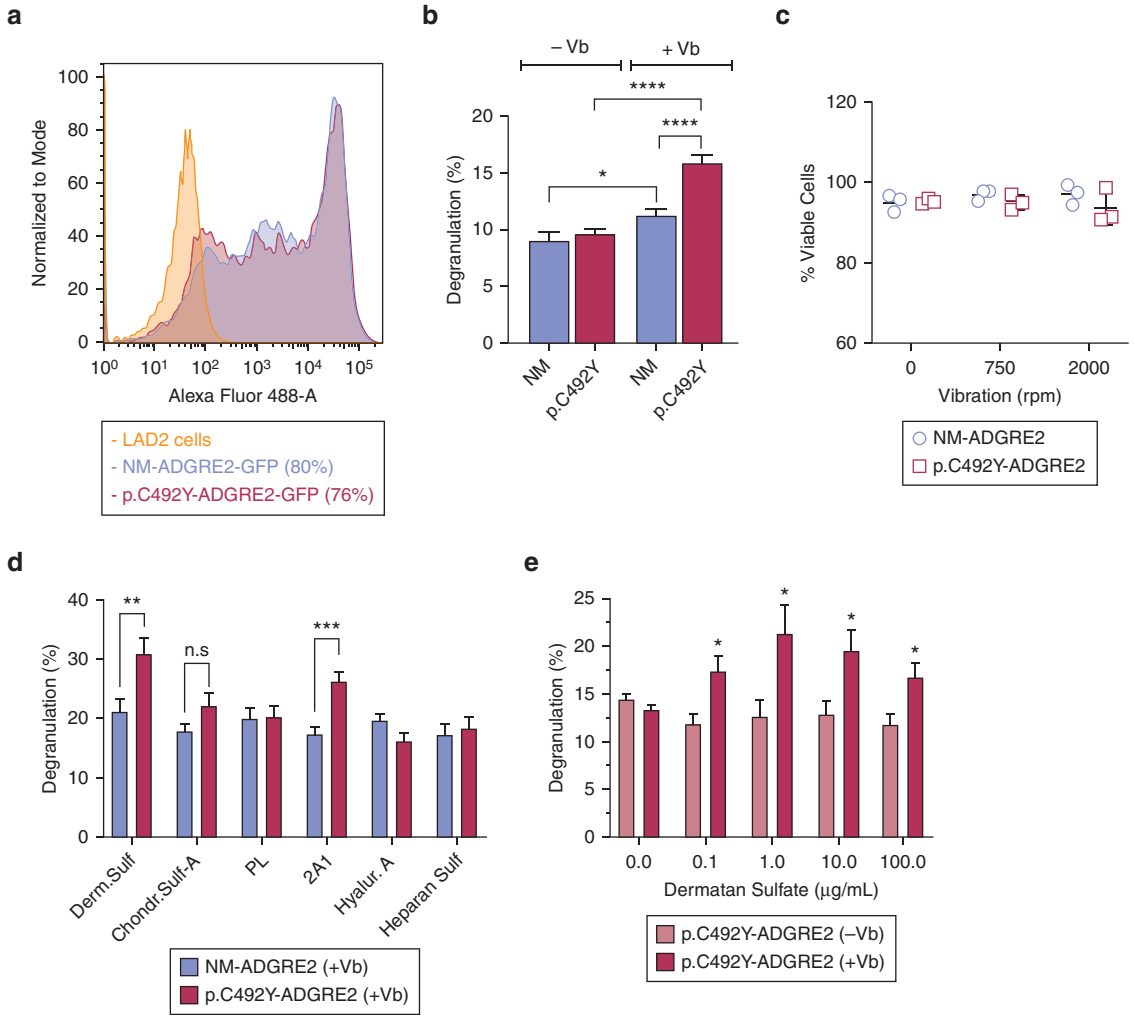

Supplementary Figure S1. Efficiency of transfection for normal and mutated ADGRE2, and characteristics of vibration-induced degranulation. (**a**) LAD2 cells were transfected with NM-ADGRE2-GFP or p.C492Y-ADGRE2-GFP and 20 hours later, efficiency of transfection was determined by FACS. (**b**) β-Hexosaminidase release in response to vibration. Cells were plated in DS-coated dishes and subjected or not to Vb(750 r.p.m.) for 20 minutes. Data are mean ± SEM (n > 30). (**c**) Effect of Vb on cell viability. Cells were collected after Vb (20 minutes) and stained with acridine orange (stains all cells in green) and propidium iodide (stains dead cells in red). Viable and dead cells were counted using a dual fluorescence Cell Counter (Luna-FL). (**d**) Effect of ADGRE2 ligation to stated substrates on Vb-induced degranulation. NM-ADGRE2 or p.C492Y-ADGRE2 cells were plated on wells coated with DS (100 µg/ml), chondroitin sulfate A (100 µg/ml), polylysine (PL; 0.01%), 2A1 monoclonal antibody (50 µg/ml), hyaluronic acid (100 µg/ml), or heparan sulfate (100 µg/ml). (**e**) Degranulation of p.C492Y-ADGRE2 plated on the indicated concentrations of immobilized DS with or without vibration. In **b**, **d**, and **e**, cells were vibrated for 20 minutes at 750 r.p.m., and degranulation was measured by β-hexosaminidase release. Data are mean ± SEM (n ≥ 7). *$P < 0.05$; **$P < 0.01$; ***$P < 0.001$; ****$P < 0.0001$. AU, arbitrary units; DS, dermatan sulfate; LAD_2, laboratory of allergic diseases-2 mast cell line; NM, nonmutated; n.s., not significant; Vb, vibration.

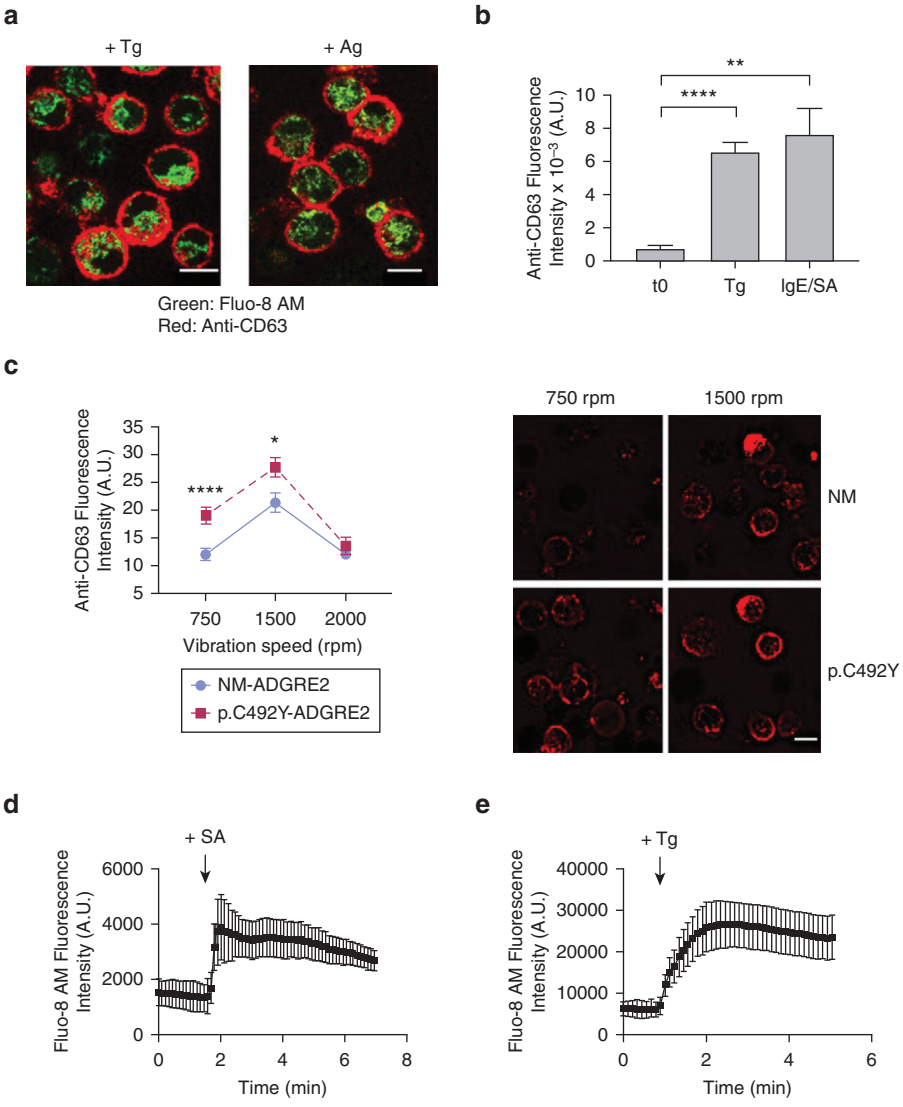

Supplementary Figure S2. Degranulation and calcium changes induced by thapsigargin or by stimulation of the high-affinity IgE receptor using confocal microscopy. (**a**) Degranulation and calcium mobilization induced by 1 μM Tg or through stimulation of the high-affinity IgE receptor (IgE/SA). Confocal images show the changes in fluorescent intensity of Fluo-8 AM (changes in intracellular calcium) and anti−CD63-APC (degranulation). Bar = 10 μm. (**b**) Quantification of CD63 exposure after activation with Tg or IgE/SA. For IgE receptor stimulation, LAD2 cells were sensitized with biotinylated IgE overnight and washed before loading with Fluo-8 AM. Cells were then challenged with 100 ng/ml of SA. Anti−CD63-APC was added immediately after stimulation and fluorescent intensity was quantified 10 minutes later. (**c**) Effect of the Vb strength on CD63 cell surface exposure of NM-ADGRE2 and p.C492Y-ADGRE2 cells. Shown is anti−CD63-APC fluorescent intensity 10 minutes after vibration in responding cells (with signals above background fluorescence). Scale bar = 10 μm. Data quantification at 2,000 r.p.m. was not reliable because cells significantly detached and cell integrity was also partly compromised. This contrasts with the β-hexosaminidase release experiments (done in round wells) where no effects in viability or cell numbers were detected (see Supplementary Figure S1c), which we believe relates to the different size and geometry of the chambers. (**d, e**) Changes in intracellular calcium induced by stimulation of the (**d**) high-affinity IgE receptor or by (**e**) Tg measured by Fluo-8 using confocal microscopy. Data represent mean ± SEM, n = 5. $^{**}P < 0.005$ and $^{****}P < 0.0001$. AM, acetoxymethyl ester; APC, allophycocyanin; DS, dermatan sulfate; LAD_2, laboratory of allergic diseases-2 mast cell line; NM, nonmutated; SA, streptavidin; Tg, thapsigargin; Vb, vibration.

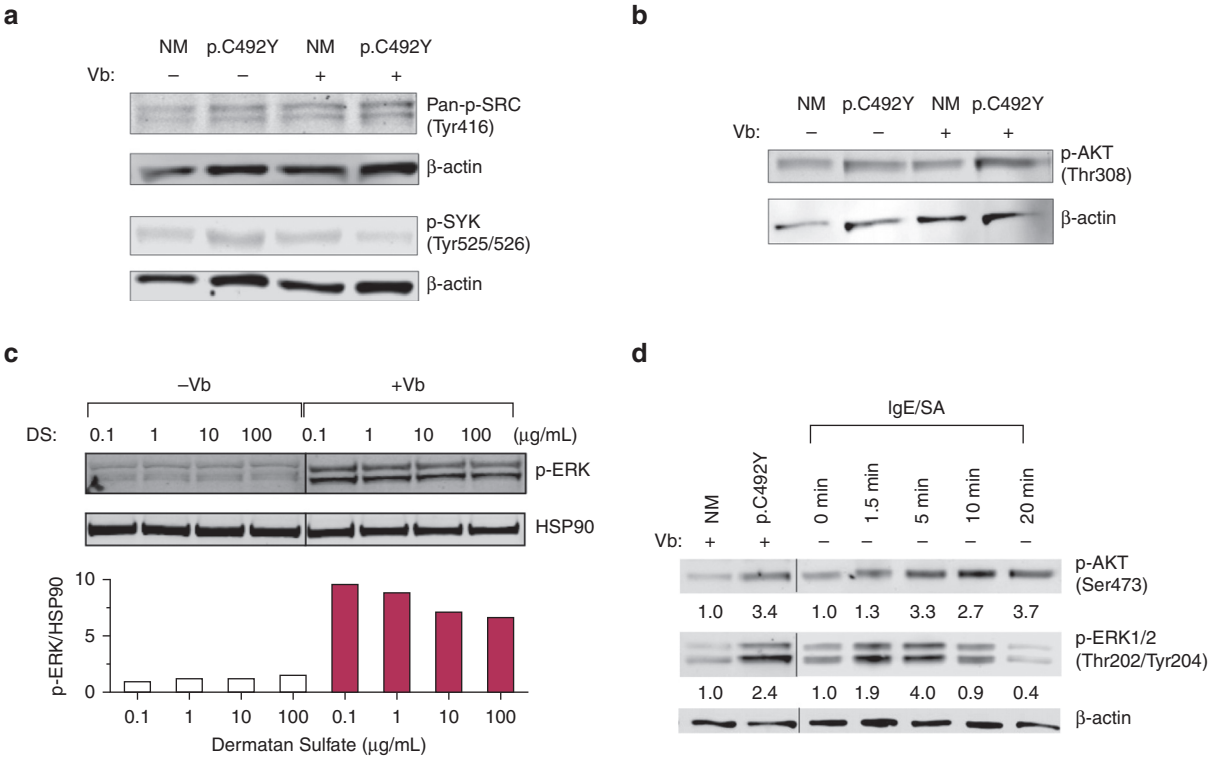

Supplementary Figure S3. Vibration does not activate Src or SYK but induces similar Akt and ERK1/2 phosphorylation to that mediated by IgE receptor stimulation. DS-bound LAD2 cells expressing NM-ADGRE2 or p.C492Y-ADGRE2 were vibrated (+Vb) for 5 minutes at 750 r.p.m. Cell lysates were then obtained and resolved in SDS-PAGE. (**a**) Phosphorylation in Src family members and SYK. (**b**) Akt phosphorylation in Thr308, a target for PDK1. Blots are from a representative experiment of at least three different experiments. (**c**) ERK1/2 phosphorylation after Vb of p.C492Y-ADGRE2 cells on DS-coated plates at the indicated concentrations. The histogram shows the quantification of band intensities (normalized by HSP90) and expressed as fold change compared with nonvibrated, NM-ADGRE2 cells plated in 0.1 μg/ml DS. (**d**) Comparison of the extent of Akt and ERK1/2 phosphorylation induced by vibration or activation by the IgE receptor on nonattached cells, done side by side. For IgE receptor stimulation, LAD2 cells were sensitized with biotinylated IgE overnight, washed, and challenged with 100 ng/ml SA. AKT, protein kinase B; DS, dermatan sulfate; ERK, extracellular signal–regulated kinase; LAD_2, laboratory of allergic diseases-2 mast cell line; NM, nonmutated; PDK1, phosphoinositide dependent kinase 1; SA, streptavidin; SYK, spleen tyrosine kinase; Vb, vibration.

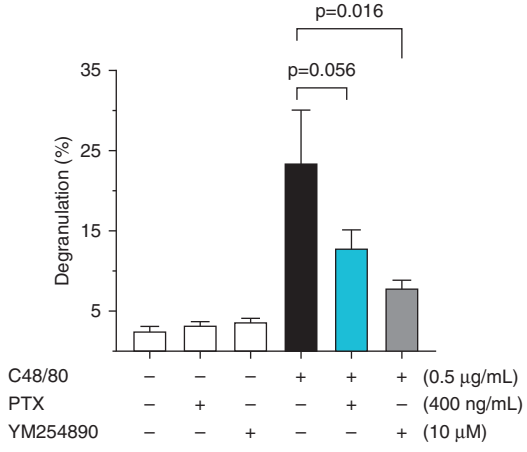

Supplementary Figure S4. Degranulation induced by MRGPRX2 in LAD2 cells is partially inhibited by PTX or YM254890. LAD2 cells were stimulated for 30 minutes with compound 48 of 80 (0.5 μg/ml), a ligand for the GPCR involved in pseudoallergic responses, MRGPRX2. Cells were pretreated for 20 minutes with or without PTX to inhibit $\alpha_{i/o}$-mediated signaling or YM254890 to inhibit $\alpha_{q/11/14}$. Degranulation was determined as the percentage of β-hexosaminidase released into the media compared with total cellular content. LAD_2, laboratory of allergic diseases-2 mast cell line; GPCR, G-protein coupled receptors; PTX, pertussis toxin.